*particles*

MDPI

*Review*

# Radiative Decays of Hadronic Molecules: From Confusion to Inspiration

**Feng-Kun Guo [1,2,*], Christoph Hanhart [3] and Alexey Nefediev [4]**

[1] Institute of Theoretical Physics, Chinese Academy of Sciences, Beijing 100190, China
[2] School of Physical Sciences, University of Chinese Academy of Sciences, Beijing 100049, China
[3] Institute for Advanced Simulation, Forschungszentrum Jülich, D-52425 Jülich, Germany; c.hanhart@fz-juelich.de
[4] Helmholtz-Institut für Strahlen- und Kernphysik, Universität Bonn, D-53115 Bonn, Germany; a.nefediev@uni-bonn.de
* Correspondence: fkguo@itp.ac.cn

**Abstract**

Radiative decays of hadronic states provide an essential source of information that can facilitate deciphering their nature and properties. However, a lot of confusion concerning radiative decays of hadronic molecules and their interpretation can be found in the literature. In this paper, we briefly review several types of such decays and pinpoint similarities and essential differences between them. In particular, we emphasise the crucial role played by the hierarchy of the scales relevant to the studied system and the resulting necessity of employing an approach that considers them appropriately. We illustrate the situation with several instructive examples.

**Keywords:** radiative decays; hadronic molecules; wave function

## 1. Introduction

The emission of photons is governed by Quantum Electrodynamics (QED), which is the simplest and most studied field theory within the Standard Model (SM). For this reason, radiative decays of hadronic states are considered a promising tool to investigate the hadrons in the initial and final states of the reaction and shed light on their nature and properties. In particular, such decays can provide access to the inner structure of these hadrons. However, the information provided by radiative decays requires care in interpretation to avoid false conclusions. In this paper, we review several examples of radiative decays of hadronic molecules and pinpoint various peculiarities related to them. In particular, we discuss the hierarchy of internal scales that can be different for different molecules and address the impact of the compact component of the wave function of the molecular state on its radiative decays.

This paper is organised as follows: In Section 2, we start from a textbook example of the two-photon decay of parapositronium and argue that the famous "universal" formula for this decay width expressed in terms of the wave function at the origin, $\psi(0)$, does not apply to hadronic molecules—states generated by the non-perturbative, strong interactions of hadron pairs; see ref. [1] for a review. We introduce and discuss an alternative expression for the width derived in the limit of zero-ranged interactions, consistent with the hierarchy of scales relevant for such hadronic molecules, and demonstrate that the derived formula works very well for two-photon decays of the scalar mesons $a_0/f_0(980)$ treated as $K\bar{K}$ molecules. Then, in Section 3, we address the radiative decays of $\phi(1020)$ that also involve



Academic Editors: Zhu-Fang Cui and Craig Roberts

Received: 19 March 2026
Accepted: 20 April 2026
Published: 28 April 2026

the above scalars in the final state. We argue that a proper treatment of the diagrams and the molecular vertex consistent with quantum mechanics and gauge invariance allows one to arrive at a reliable finite prediction for the decay width. In Section 4, we proceed to the radiative decays of the $D_{s1}(2460)$ meson treated as a $D^*K$ molecule. In this case, although the loop amplitudes do not diverge, it follows from the power counting that there is no enhancement of the loop diagrams compared with the contact term, so the corresponding contact amplitude needs to be included. Thus, the radiative decays of the $D_{s1}(2460)$ meson provide an example of the situation when an additional experimental input is necessary to fix the unknown short-range parameter and this way to arrive at a complete theory capable of providing definite predictions for observables. A ratio of the branching fractions of two radiative decays of the $D_{s1}(2460)$, if measured experimentally, is argued to be able to provide such an input. Finally, in Section 5, we turn to the radiative decays of the $X(3872)$, also known as $\chi_{c1}(3872)$, as yet another prominent candidate for a hadronic molecule, and argue that the divergence of the loop amplitudes contributing the decays $X \to \gamma\psi$ ($\psi = J/\psi, \psi(2S)$) calls for the inclusion of the leading-order short-range contact term that is further found to strongly depend on the renormalisation scale. It is concluded, therefore, that the radiative decays of the $X(3872)$ are mostly sensitive to the short-range component of its wave function and as such are not decisive in probing the molecular nature of the $X$. We conclude in Section 6.

## 2. Positronium Versus a Point-like Molecule

We start from two-photon decays of parapositronium as the most prominent example of the radiative decay of a compound state. Parapositronium is a bound state of the electron–positron pair with the quantum numbers $^1S_0$. In what follows we also refer to it as Ps($^1S_0$) or simply "positronium". Given its positive $C$-parity, parapositronium decays into an even number of photons, the two-photon decay being the dominant one. Two features inherent in the positronium make it a distinct object for studies. On the one hand, it is undoubtedly a composite system represented by a generic bound state. On the other hand, the interaction responsible for its binding is very well understood—the bound state is formed by the attractive Coulomb potential and can be readily found as a solution of the corresponding Schrödinger equation with the ground state wave function and binding momentum being (the meaning of the subscript $A$ will be explained below)

$$\psi_A(r) = \sqrt{\frac{\gamma^3}{\pi}}\, e^{-\gamma r}, \quad \gamma = \sqrt{2\mu_e E_B}\,, \tag{1}$$

respectively, where

$$\gamma = \alpha\mu_e \quad \text{and} \quad \mu_e = \frac{m_e^2}{m_e + m_e} = \frac{1}{2}m_e\,, \tag{2}$$

with $m_e$ being the electron mass and $\alpha = e^2/(4\pi) \approx 1/137$ the electromagnetic fine structure constant. Hereinafter we use the symbol $\mu$ for the relevant reduced mass. Then, according to textbooks in quantum mechanics, the width of a two-photon decay of the positronium can be evaluated as

$$\Gamma[\text{Ps}(^1S_0) \to \gamma\gamma] = v\rho\sigma, \tag{3}$$

where $v$ is the velocity of the electron (positron) in the positronium rest frame, $\rho = |\psi_A(0)|^2$ is the probability of the electron and positron meeting each other at the origin (annihilation point), and

$$\sigma = \frac{4\pi\alpha^2}{m_e^2 v} \tag{4}$$

is the total cross section of the two-photon annihilation of a slow $e^+e^-$ pair in the $^1S_0$ state. Combining Equations (1)–(4), it is easy to arrive at the famous formula

$$\Gamma[\mathrm{Ps}(^1S_0)] = \frac{4\pi\alpha^2}{m_e^2}|\psi_A(0)|^2 = \frac{1}{2}\alpha^5 m_e\,. \tag{5}$$

The corrections to Equation (5) are suppressed by higher powers of the fine structure constant $\alpha$.

The simplicity and the seemingly universal form of Equation (5) have made it an extremely popular and de facto default approach to two-photon decays of compound objects. For example, the two-photon decay of kaonium (the bound state of a kaon–antikaon pair bound by the strong force—in other words, a hadronic molecule of $K\bar{K}$) has been studied in the literature employing the above technique with results ranging from 0.6 keV [2] to 6 keV [3]. The order-of-magnitude discrepancy between these predictions should not come as a surprise given that the formula for the decay width relies on the value of the wave function at the origin, which is extremely sensitive to the details of the interaction. Since the strong interaction potential of kaons is not known at short distances, any calculation of this kind relies on a particular model, and the corresponding hardly quantifiable model uncertainty automatically propagates to the final result. However, a blind application of the positronium-like formula (5) to a generic two-photon decay of a molecule is potentially dangerous, since it relies on a particular hierarchy of scales [4]. Indeed, the positronium two-photon decay amplitude is encoded in the two diagrams depicted in Figure 1. Then taking the integral in the loop energy $p_0$, and retaining only the leading nonrelativistic contribution, one readily arrives at

$$\mathcal{M}[\mathrm{Ps}(^1S_0) \to \gamma\gamma] = \frac{1}{\sqrt{m_e}}\int \frac{d^3\boldsymbol{p}}{(2\pi)^3}\psi_A(\boldsymbol{p})\mathcal{M}[e^+e^- \to \gamma\gamma], \tag{6}$$

where $\mathcal{M}[e^+e^- \to \gamma\gamma]$ is the amplitude of an unbound electron–positron pair annihilation into two photons. Equation (6) is still general. In the case of positronium it is easy to see that the two objects under the momentum integral in the amplitude (6) possess very different typical momentum scales. While the wave function effectively cuts the integral at $p \equiv |\boldsymbol{p}| \sim \alpha m_e$, the momentum scale controlling the transition to the two photons is much larger, of the order of $m_e$, such that $\mathcal{M}[e^+e^- \to \gamma\gamma]$ stays basically constant in the momentum range, where the integral has already converged. As a result, the amplitude $\mathcal{M}[e^+e^- \to \gamma\gamma]$ can be pulled out from the integral, so the positronium coordinate-space wave function taken at the origin,

$$\psi_A(0) = \int \frac{d^3\boldsymbol{p}}{(2\pi)^3}\psi_A(\boldsymbol{p}), \tag{7}$$

arises quite naturally. Thus we conclude that the positronium-like formula (5) relies on a particular hierarchy of scales,

$$r_\Gamma \gg r_a, \tag{8}$$

with $r_\Gamma$ and $r_a$ for the typical scale of the bound state vertex and annihilation scale, respectively, which in the case of positronium are

$$r_\Gamma \simeq \frac{1}{\kappa}, \quad \text{with} \quad \kappa \simeq \alpha\left(\frac{1}{2}m_e\right) = \gamma, \tag{9}$$

and

$$r_a \simeq \frac{1}{m_e}. \tag{10}$$

Note that the case of positronium is very special, since the binding is provided by the massless photon. Accordingly, the effective range of the interaction is provided by $\mu_e\alpha$, which agrees with the binding momentum $\gamma$—clearly, for hadronic molecules where the range of the binding forces is $\mathcal{O}(m_\pi^{-1})$ or shorter, this equality is absent.

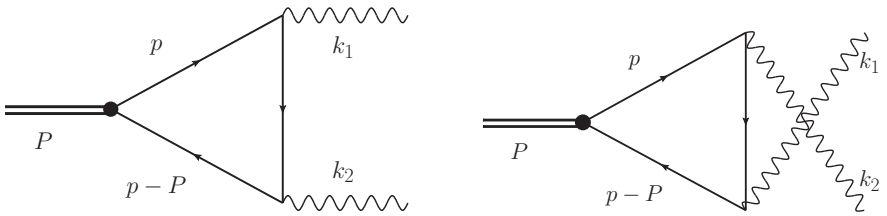


**Figure 1.** The two diagrams contributing to the two-photon decay of parapositronium. The black filled circle indicates the positronium disintegration vertex that can be obtained as solution of the Bethe-Salpeter bound-state equation and contains the positronium wave function as the central (but not only!) ingredient—see, for example, the derivation of Equation (22) in Section 3 below. The other two vertices in the diagrams are the standard photon emission vertices controlled by QED.

Hereinafter, we refer to the hierarchy of Equation (8) as case A (hence the subscript $A$ at the wave function) or the "positronium" limit. In this limit, the disintegration of the molecule into its constituents effectively takes place at the origin—the point in space where the constituents "meet" each other with probability $|\psi_A(0)|^2$. The wave function in Equation (1) comes as solution of the Schrödinger equation with the Coulomb potential, and its Fourier transform takes the form

$$\psi_A(\boldsymbol{p}) = \frac{8\sqrt{\pi\gamma^5}}{(p^2+\gamma^2)^2}. \tag{11}$$

As indicated above, a different (opposite to case A above) hierarchy of scales is typically relevant for hadronic molecules, namely

$$r_\Gamma \ll r_a\,, \tag{12}$$

which we refer to as case B and accordingly use the corresponding subscript at the wave function. Now the interaction of the constituents responsible for the formation of the molecule is controlled by the mass of the lightest exchange particle allowed, in the following denoted as $\beta$. The extreme limit of $\beta \to \infty$ is often referred to as the "point-like" or zero-range limit, since then the molecule is formed by a zero-range potential. In this case, the bound state wave function takes the form

$$\psi_B(r) = \sqrt{\frac{\gamma}{2\pi}}\frac{1}{r}e^{-\gamma r}, \quad \gamma = \sqrt{2\mu E_B}, \quad \mu = \frac{m_1 m_2}{m_1+m_2} \tag{13}$$

in coordinate space, or

$$\psi_B(\boldsymbol{p}) = \frac{\sqrt{8\pi\gamma}}{p^2+\gamma^2}, \tag{14}$$

in momentum space. More generally, Equation (13) describes the long-distance tail of the wave function outside the range where the interaction potential is different from zero. As such this wave function is universal, since it does not depend on the details of the particular potential employed in the corresponding Schrödinger equation at short range. It can be obtained as a solution of the Schrödinger equation in the potential $\delta^{(3)}(\boldsymbol{r})$. However, in reality it gets modified for distances of the order of the range of forces or lower—a regime that in effective field theories is largely parametrised by local operators (see ref. [5] for a related discussion). The fact that the wave function in Equation (13) diverges in the limit

$r \to 0$ does not cause trouble in the pertinent calculations, since the positronium formula for the width in Equation (5) that involves $\psi(0)$ does not apply as soon as the interaction is of a shorter range than the transition of the constituents to the final state. The described situation is always realised in the point-like limit, such that in case B the two-photon decay width of a molecule of mass $M$ is calculated as [4]

$$\Gamma_{\gamma\gamma}(\beta) = \Gamma_{\gamma\gamma}\left(1 + \mathcal{O}\left(\frac{mE_B}{\beta^2}\right)\right), \qquad E_B = 2m - M, \tag{15}$$

where

$$\Gamma_{\gamma\gamma} = \Gamma_{\gamma\gamma}(\beta \to \infty) = \zeta^2 \left(\frac{\alpha}{\pi}\right)^2 \sqrt{mE_B}\left(\frac{2m}{M}\right)\left[\left(\frac{2m}{M}\right)^2 \arcsin^2\left(\frac{M}{2m}\right) - 1\right]^2, \tag{16}$$

and the factor $\zeta \leqslant 1$ accounts for the fact that not all constituents of the molecule (for example, neutral hadrons) may participate in the decay. The expression above is provided for $m_1 = m_2 = m$ to simplify the formula. Importantly, it was argued on general grounds and demonstrated explicitly in ref. [4] that potentially sizable corrections of the order $\mathcal{O}(m^2/\beta^2)$ to the point-like formula in Equation (16) cannot appear. Importantly, the width in Equation (16) comes as a result of the straightforward evaluation of the loop amplitude that acquires three contributions: two of them taking the form of the diagrams in Figure 1 plus a contact diagram depicted in Figure 2 that appears for gauge theories of charged spinless particles interacting with photons as well as for charged nonrelativistic particles with spin. The molecular vertex is in an $S$-wave, so it does not introduce any loop momentum, and the corresponding coupling constant can be evaluated in terms of the binding momentum—see Equation (22) below. Thus, all photon emission vertices in the diagrams are electric ones. Then the gauge invariance of the amplitude leads to delicate cancellations between different terms coming from the above three diagrams and is only in place if all three contributions to the amplitude are retained. Those cancellations at the same time remove the divergent pieces from the amplitude, such that the total amplitude is ultraviolet (UV) finite, while its individual (gauge non-invariant!) parts are divergent. Indeed, gauge invariance forces internal loop momenta to get converted into external momenta, this way improving the UV behaviour of the integrated function, to allow for a transverse tensor structure of the total amplitude.

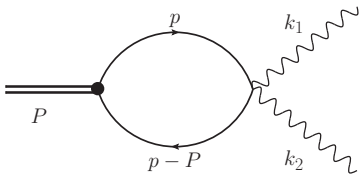


**Figure 2.** Contact diagram that contributes to the amplitude of the two-photon decay of a composite object composed of two charged scalar (or pseudoscalar) particles.

The formulae in Equations (15) and (16) apply to the case of the two-photon decays of the scalar $f_0(980)$ treated as a $K\bar{K}$ molecule. Indeed, the relevant scales in this case are

$$r_\Gamma \simeq \frac{1}{\beta} \simeq \frac{1}{m_\rho}, \quad r_a \simeq \frac{1}{m_K}, \tag{17}$$

with $m_\rho \approx 770$ MeV and $m_K \approx 490$ MeV. In Equation (17) the pion exchange between pseudoscalar kaons is forbidden by parity conservation, so the lightest allowed exchange particle is the $\rho$ meson. The hierarchy of the scales in Equation (17) is obviously at odds

with case A in Equation (8) and the two-photon decay of a $K\bar{K}$ molecule rather falls into class B as given by Equation (12). Then Equations (15) and (16) give for the width [4]

$$\Gamma^{\rm th}_{\gamma\gamma}[f_0(980)] = (0.22 \pm 0.07)\ \text{keV}, \tag{18}$$

where $m_S = 980$ MeV was used that, together with the kaon mass quoted above, translates into the binding energy $E_B = 10$ MeV. It was also taken into account that, in case of $f_0(980)$, only the charged kaons in the loop couple to the photons in leading order, so $\zeta^2 = 1/2$. The uncertainty was estimated from the size of the leading neglected correction $\mathcal{O}(mE_B/\beta^2)$ in Equation (15), with $\beta = m_\rho$, as given in Equation (17). The result in Equation (18) is consistent with the experimental measurement by Belle [6],

$$\Gamma^{\rm exp}_{\gamma\gamma}[f_0(980)] = 0.205^{+0.095}_{-0.083}(\text{stat})^{+0.147}_{-0.117}(\text{syst})\ \text{keV}. \tag{19}$$

In summary, we stress that the appropriate approach to two-photon decays of composite systems crucially depends on the hierarchy of the scales responsible for the formation of the state and the annihilation of its constituents to a pair of photons. Since the zero-range potential often provides a valid approximation for the binding interaction of hadronic molecules, a positronium-like treatment, Equation (8), is not justified and the point-like limit of Equation (12) should be used instead. In the latter case, the result for the decay width is not sensitive to the details of the interaction at short distances and only depends on the long-range tail of the molecule wave function that is model-independent. In case of a $K\bar{K}$ molecule, the loop integral converges in the point-like limit as a result of the gauge invariance of the photon vertices. In particular, no short-range operator needs to be added at leading order, since the kaon loops provide the dominating contribution to the decay amplitude. Therefore, the result in Equation (18) comes as a theoretical prediction for the two-photon decay of the $K\bar{K}$ molecule that depends only on the masses of the decaying state and its constituents.

## 3. Radiative Decays of $\phi(1020)$

The processes $\phi(1020) \to \gamma a_0/f_0(980)$ constitute yet another example of radiative decays involving the scalar mesons $a_0/f_0(980)$. They are studied in refs. [7,8] and a conclusion is made that, for the scalars treated as $K\bar{K}$ molecules with the radial wave function in Equation (11), the $\phi(1020)$ radiative decay rates are strongly suppressed in comparison with the case of compact scalars. In addition, the authors of refs. [8,9] claim that the integrals in the corresponding loop amplitudes in Figure 3 are sensitive to very large (of the order of GeVs) loop momenta and, therefore, $a_0/f_0(980)$ need to be interpreted as compact tetraquark states rather than extended hadronic molecules. These findings and conclusions are scrutinised and criticised in refs. [10,11], so below we briefly mention the arguments put forward in the latter works that are in line with the discussion above.

It was shown in the previous section that the scalars $a_0/f_0(980)$ treated as $K\bar{K}$ molecules comply with the hierarchy of the relevant scale in Equation (12) rather than Equation (8), so the choice of the wave function in the form of $\psi_A(\boldsymbol{p})$ in Equation (11) is not justified. As a next step we derive the molecule disintegration vertex and notice that, in the vicinity of a bound state, the nonrelativistic $t$-matrix takes the form

$$t(\boldsymbol{p}, \boldsymbol{p}', E) = \frac{f(\boldsymbol{p}) f(\boldsymbol{p}')}{E + E_B - i0}, \tag{20}$$

where the nonrelativistic vertex $f(\boldsymbol{p}) = \hat{v}\psi_B(\boldsymbol{p})$ (here $\psi_B(\boldsymbol{p})$ is the wave function in Equation (14) and $\hat{v}$ is the nonrelativistic interaction operator) can be found directly from the Schrödinger equation in momentum space,

$$\frac{\boldsymbol{p}^2}{2\mu}\psi_B(\boldsymbol{p}) - \hat{v}\psi_B(\boldsymbol{p}) = -E_B\psi_B(\boldsymbol{p}), \tag{21}$$

with $E_B = \gamma^2/(2\mu)$, that gives a constant nonrelativistic vertex,

$$f(\boldsymbol{p}) = \frac{1}{2\mu}(\boldsymbol{p}^2 + \gamma^2)\psi_B(\boldsymbol{p}) = \frac{\sqrt{8\pi\gamma}}{2\mu}, \tag{22}$$

in agreement with the point-like limit introduced in the previous section and the famous Weinberg formula for the molecule coupling to its constituents [1,12]. Explicit calculations performed in ref. [10] demonstrate that, for a realistic set of parameters, there is no suppression of the decay rates $\phi(1020) \to \gamma a_0/f_0$ for the scalar mesons regarded as molecules, and the deviations from the point-like limit caused by a residual momentum dependence of the molecular vertex have only very little effect on the result. It needs to be noted that, similarly to the case of the two-photon decay of a molecule addressed in the previous section, the photon is emitted from electric vertices and the individual loop diagrams in Figure 3a–c lead to divergent integrals but the full amplitude that sums these contributions is finite. Moreover, contrary to the claim in refs. [9,13], after a proper treatment of the individual contributions to the amplitude, the resulting loop integral converges at nonrelativistic momenta—again a direct consequence of gauge invariance. We therefore conclude that the data for the scalars $a_0/f_0(980)$ in the final state of the $\phi(1020)$ radiative decay are consistent with these enigmatic states being pure $\bar{K}K$ molecular states.

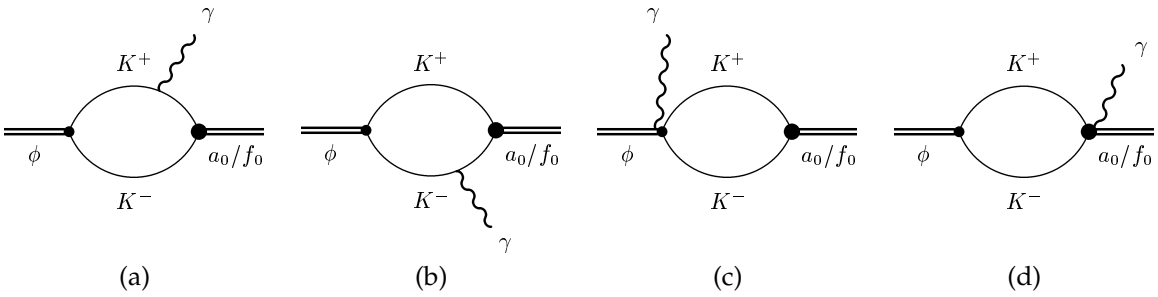


**Figure 3.** Loop diagrams contributing to the radiative decays $\phi(1020) \to \gamma a_0/f_0(980)$. The diagrams (**a**–**c**) are from the minimal coupling. Diagram (**c**) guarantees gauge invariance of the total amplitude while diagram (**d**) appears only when proceeding beyond the strict point-like limit for the vertex $K\bar{K} \to a_0/f_0$. Adapted from ref. [10].

## 4. Radiative Decays of $D_{s1}(2460)$

In this section, we review the radiative decays of the $D_{s1}(2460)$. We start from the two-body decay $D_{s1}(2460) \to \gamma D^*_{s0}(2317)$ assuming dominating molecular components in the wave functions of both $D_{sJ}$ mesons involved [14–21]. The effective Lagrangian describing this decay takes the form

$$\mathcal{L}_{\text{eff}} = \kappa\varepsilon^{\mu\nu\alpha\beta}F_{\mu\nu}v_\beta D_{s1\alpha}D^{*\dagger}_{s0} + \text{h.c.}, \tag{23}$$

where $v$ denotes the 4-velocity of the $D_{s1}$ meson and $\kappa$ represents a dimensionless effective coupling constant. Notice that an alternative identification of $v$ as the 4-velocity of the decaying $D^*_{s0}$ meson would only affect subleading terms in the heavy quark mass expansion that can be neglected. Then the decay width is calculated as

$$\Gamma[D_{s1} \to \gamma D^*_{s0}] = \frac{\kappa^2\omega^3}{3\pi m^2_{D_{s1}}}, \tag{24}$$

where $\omega \approx 139$ MeV is the energy of the photon.

Formally, the decay $D_{s1}(2460) \to \gamma D^*_{s0}(2317)$ proceeds through the diagrams shown in Figure 4. We study the loop amplitude first and notice that (i) the molecular vertices $D_{s1} \to D^*K$ and $D^*_{s0} \to DK$ are $S$-wave ones, so they do not bring powers of the loop momentum and (ii) the coupling constants can be evaluated either from the corresponding binding energies using the well-known Weinberg formula [12] or from the residues of the scattering amplitudes in the unitarised chiral perturbation theory (UChPT) that generates the $D^*_{s0}$ and $D_{s1}$ mesons dynamically. In addition, the magnetic photon emission vertex $D^* \to \gamma D$ is also well understood and its parameters can be extracted directly from the experimental data on the corresponding radiative decay. Then, as discussed in ref. [22], the momentum-dependent effective loop coupling $\kappa_{\rm loop}(q^2)$ coming from the loop diagram in Figure 4 can be evaluated straightforwardly since the corresponding loop amplitude involves only convergent integrals. It is instructive to note that, in this case, gauge invariance (and UV-finiteness) of the loop amplitude is guaranteed by the anomalous coupling in the effective Lagrangian (23) and the magnetic photon emission vertex $D^* \to \gamma D$ that is by construction transverse with respect to the photon momentum. In particular, here the subtle cancellations discussed above do not take place. For a realistic set of parameters, $\kappa_{\rm loop}(q^2)$ evaluated on the mass shell of the $D^*_{s0}$ reads [22]

$$\kappa_{\rm loop}(q^2 = m^2_{D^*_{s0}}) \approx 0.19. \tag{25}$$

The momentum dependence of $\kappa_{\rm loop}(q^2)$ is depicted in Figure 5, with the result in Equation (25) shown by the vertical dashed-dotted line.

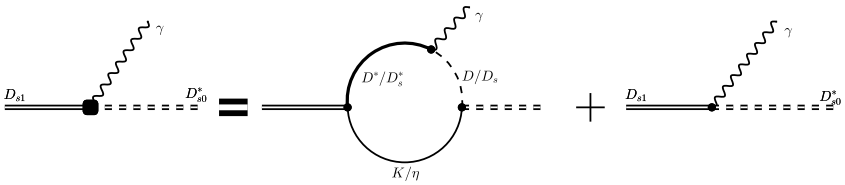


**Figure 4.** The loop and contact diagrams contributing to the radiative decay $D_{s1}(2460) \to \gamma D^*_{s0}(2317)$. Adapted from [22].

As argued in ref. [23] and contrary to the hadronic decays of the $D_{s1}(2460)$, there is no enhancement of the loop diagrams compared with the contact term in its radiative decay. Then the full coupling $\kappa$ in Equation (24) acquires two contributions,

$$\kappa = \kappa_{\rm loop}(q^2 = m^2_{D^*_{s0}}) + \kappa_{\rm cont}, \tag{26}$$

where the term $\kappa_{\rm cont}$ sets the strength of the contact diagram in Figure 4. The value of $\kappa_{\rm cont}$ is currently unknown and was estimated in ref. [22] in two ways. On the one hand, Equation (24) was applied to a quark-model result for the decay width of a generic $c\bar{s}$ state, $\Gamma[1^+(c\bar{s}) \to 0^+(c\bar{s}) + \gamma] \approx 2.74$ keV [24], to find

$$|\kappa_{\rm cont}| \simeq 0.24. \tag{27}$$

On the other hand, the exciting experimental data on the radiative decay $D_{s1}(2460) \to \gamma D^*_{s0}(2317)$ [25] and theoretical estimates for various $D_{s1}(2460)$ partial decay widths were employed to get [22]

$$\kappa_{\rm cont} \simeq 0.2. \tag{28}$$

Remarkably, the numerical estimates in Equations (27) and (28) comply well with both a natural expectation $\kappa_{\rm cont} \simeq \Lambda_{\rm QCD}/m_c \simeq 0.2$, coming from the fact that the consid-

ered decay involves a heavy quark spin flip, and the power counting argued in ref. [26], thus yielding

$$|\kappa_{\rm cont}| \simeq |\kappa_{\rm loop}(q^2 = m^2_{D^*_{s0}})|. \tag{29}$$

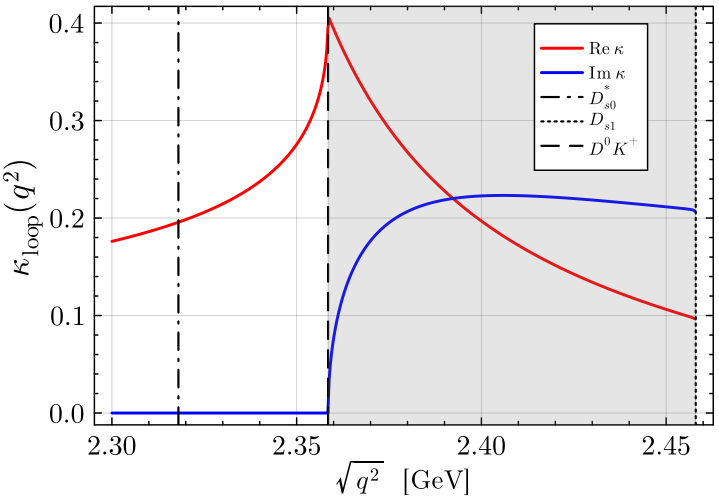


**Figure 5.** The momentum dependence of the effective loop coupling $\kappa_{\rm loop}(q^2)$, as an example, evaluated for the masses of $D^{(*)+}$ and $K^0$. The vertical dashed-dotted line shows the position of $q^2 = m^2_{D^*_{s0}}$ relevant for the two-body decay $D_{s1}(2460) \to \gamma D^*_{s0}(2317)$. The gray band shows the range of the phase space integration in the three-body decay $D_{s1}(2460) \to \gamma D^0 K^+$, $(m_{D^0} + m_{K^+})^2 \leqslant q^2 \leqslant m^2_{D_{s1}}$. Adapted from ref. [22].

Then indeed, as anticipated in ref. [23], different models for the structure of the $D_{s1}$ meson may lead to similar results for its radiative decay width. However, the result in Equation (27) is strongly model-dependent while, given the very poor knowledge of the experimental branching $\mathrm{Br}(D_{s1}(2460) \to \gamma D^*_{s0}(2317))$, the estimate in Equation (28) comes with a large uncertainty, around 100%. Thus, more reliable and accurate methods to evaluate $\kappa_{\rm cont}$ need to be invoked. In particular, it is argued in ref. [22] that the value of the contact contribution $\kappa_{\rm cont}$ could be extracted from the ratio

$$\mathcal{R}_{D_{s1}} = \frac{\mathrm{Br}(D_{s1}(2460) \to \gamma D^*_{s0}(2317))}{\mathrm{Br}(D_{s1}(2460) \to \gamma D^0 K^+)} \tag{30}$$

that demonstrates a lively dependence on this parameter. The amplitude for the transition $D_{s1}(2460) \to \gamma D^*_{s0}(2317)$ enters the amplitude for the three-body decay $D_{s1}(2460) \to \gamma D^0 K^+$ as a substructure (see Figure 6b) and in this way gives it a dependence on $\kappa_{\rm cont}$. Experimental determination of the ratio in Equation (30) or at least imposing a constraint on its value, which is easier than measuring the involved partial decay widths separately, may already be sufficient to arrive at a fair estimate for $\kappa_{\rm cont}$. Furthermore, as found in ref. [22], the width of the three-body radiative decay $D_{s1}(2460) \to \gamma D^0 K^+$ is sensitive to the loop coupling $\kappa_{\rm loop}(q^2)$ evaluated in a different kinematical regime compared with the two-body decay $D_{s1}(2460) \to \gamma D^*_{s0}(2317)$—see the gray shaded band in Figure 5. It is, therefore, further argued in ref. [22] that experimental studies of this three-body radiative decay may shed light on the internal structure of the $D_{sJ}$ mesons involved.

We therefore conclude this section noting that the radiative decays of the $D_{s1}(2460)$ are sensitive to both the long-range molecular and short-range compact components of its wave function which can potentially be quantified if sufficiently accurate experimental data become available.

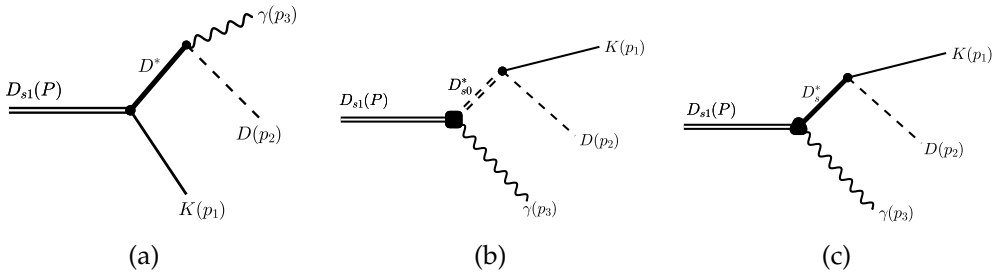


(a) (b) (c)

**Figure 6.** Various contributions to the decay amplitude $D_{s1} \to \gamma DK$. The structure of the vertex $D_{s1} \to \gamma D^*_{s0}$ in diagram (**b**) is shown in Figure 4. Details concerning the vertex $D_{s1} \to \gamma D^*_s$ in diagram (**c**) can be found in refs. [23,26,27]. Adapted from ref. [22]; see this reference also for a detailed investigation of the corresponding amplitude.

## 5. Radiative Decays of the $X(3872)$

In this section, we discuss the radiative decays $X(3872) \to \gamma\psi(2S)$ and $X(3872) \to \gamma J/\psi$ that, in recent years, have attracted a lot of attention from both experimentalists and theorists. Interest in these decays was recently catalysed by the improved analysis performed by the LHCb Collaboration. In particular, it provided the most precise measurement so far of the ratio

$$\mathcal{R}_X = \frac{\mathrm{Br}(X(3872) \to \gamma\psi(2S))}{\mathrm{Br}(X(3872) \to \gamma J/\psi)} \tag{31}$$

that reads [28]

$$\mathcal{R}_X^{\mathrm{LHCb}} = 1.67 \pm 0.21 \pm 0.12 \pm 0.04 \tag{32}$$

and supersedes the previous, 10-year-old result belonging to the same collaboration [29]. The ratio in Equation (31) has been under intensive discussion in the literature starting from its first experimental measurement by the BaBar Collaboration in 2008 [30]. Since then, several attempts have been undertaken to improve on this value (see Table 1 for a collection of the measurements belonging to various experimental groups), and the recent measurement by LHCb in Equation (32) indeed considerably advances the experimental situation.

From the theory side, shortly after the $X(3872)$ discovery by the Belle collaboration in 2003 [31], the ratio of its radiative decays in Equation (31) was argued to provide a decisive selection rule to discriminate between different assignments for the nature of the $X$ [32]. In particular, for this state interpreted as a pure $D\bar{D}^*$ molecule, the cited work reported the expectation $\mathcal{R}_X \ll 1$ at odds with most of the experimental results in Table 1. Shortly after the updated LHCb analysis in ref. [28] was announced, a tiny ratio $\mathcal{R}_X$ for a molecular $X(3872)$ was argued for in ref. [33], based on the estimates of the overlaps of various wave functions with the molecular wave function taken to be the asymptotic long-distance form as in Equation (13). This leads to the conclusion that the recent LHCb measurement precludes a molecular nature of the $X(3872)$. After some general remarks concerning the $X(3872)$, we demonstrate below that these claims are at odds with the general discussion presented in the previous sections.

**Table 1.** Experimental measurements of the ratio $\mathcal{R}_X$ in Equation (31) for the $X(3872)$ radiative decays widths.

| BaBar [30] | Belle [34] | LHCb (Old) [29] | BESIII [35] | LHCb (New) [28] |
|---|---|---|---|---|
| $3.4 \pm 1.4$ | $<2.1$ | $2.46 \pm 0.64 \pm 0.29$ | $<0.59$ | $1.67 \pm 0.21 \pm 0.12 \pm 0.04$ |

Given the unambiguously established quantum numbers $1^{++}$ of the $X(3872)$ [36,37] and the proximity of its mass to the nominal neutral $D\bar{D}^*$ threshold [25], assuming a considerable molecular $D\bar{D}^*$ component in the $X$ wave function looks quite plausible.

(Hereinafter, a proper $C$-even combination of the $D\bar{D}^*$ and $\bar{D}D^*$ components is understood). Then, based on the experience gained in the previous sections, a relevant question that arises is whether the hierarchy of the intrinsic scales in the $X(3872)$ is more consistent with the positronium case in Equation (8) or the point-like limit in Equation (12). It should be noted that, unlike the system of two kaons studied above, the pion exchange is not forbidden between the $D$ and $\bar{D}^*$ mesons. Meanwhile, the $DD\pi$ vertex is still not allowed by $P$-parity conservation, so the pion-driven interaction between the $D$ and $\bar{D}^*$ proceeds in the $u$-channel, and the corresponding potential reads

$$V_\pi(\boldsymbol{p},\boldsymbol{p}') = 3\left(\frac{g_c}{2f_\pi}\right)^2 \frac{(\boldsymbol{\epsilon}\cdot\boldsymbol{q})(\boldsymbol{q}\cdot\boldsymbol{\epsilon}'^*)}{u-m_\pi^2}, \tag{33}$$

where $\boldsymbol{p}^{(\prime)}$ and $\boldsymbol{\epsilon}^{(\prime)}$ are the momenta and polarisation vectors of the $D^*$ mesons in the initial and final states, respectively, $\boldsymbol{q} = \boldsymbol{p}' - \boldsymbol{p}$ is the pion momentum and the factor 3 stems from the eigenvalue of the isospin operator $\boldsymbol{\tau}\cdot\boldsymbol{\tau}$ for an isoscalar $D\bar{D}^*$ system (we work in the strict isospin limit—for a discussion on the role of isospin violation and how to find a possibly existing isovector partner state see ref. [38]). Furthermore,

$$u - m_\pi^2 = q^2 - m_\pi^2 = (q_0^2 - \boldsymbol{q}^2) - m_\pi^2 = -\boldsymbol{q}^2 - \left(m_\pi^2 - q_0^2\right) \approx -(\boldsymbol{q}^2 + \mu_\pi^2),$$

where the recoil terms for the $D^{(*)}$ mesons were neglected by setting $q_0 = E_{\bar{D}^*} - E_D \approx m_{D^*} - m_D$ (in this way the three-body cut, discussed in some detail in ref. [39], is removed from the amplitude; however, this is not crucial for the discussion here) and an effective pion mass parameter,

$$\mu_\pi^2 = m_\pi^2 - (m_{D^*} - m_D)^2, \tag{34}$$

has appeared naturally [40–42]. Numerically $|\mu_\pi| \approx 42$ MeV and one may be tempted to deduce from this estimate that, in the $D\bar{D}^*$ system at hand, the inverse range of the force $\beta$ is given by the parameter $|\mu_\pi|$ and as such it is small compared with the other mass scales present in the system. Then, naïvely, the positronium-like hierarchy of the scales in Equation (8) should be relevant for the $X(3872)$. However, the latter conclusion is not justified. To demonstrate this, consider the central part of the pion exchange potential (33),

$$V_\pi^{\rm cent}(\boldsymbol{q}) = \left(\frac{g_c}{2f_\pi}\right)^2 \frac{\boldsymbol{q}^2}{u-m_\pi^2} = \left(\frac{g_c}{2f_\pi}\right)^2 \left(-1 + \frac{\mu_\pi^2}{\boldsymbol{q}^2+\mu_\pi^2}\right), \tag{35}$$

where the substitution $\epsilon_i\epsilon_j'^* \to \frac{1}{3}\delta_{ij}$, relevant for the central potential, was used. Since a constant potential in momentum space (coming from the term $-1$ in parentheses) turns to a zero-radius potential $\delta^{(3)}(\boldsymbol{r})$ in coordinate space, Equation (35) corresponds to an explicit separation of the short- and long-ranged contributions, and the second term in parentheses vanishes in the limit $|\boldsymbol{q}| \to \infty$. Therefore, as stressed in ref. [43], the OPE potential in the $D\bar{D}^*$ system is well defined in the sense of an effective field theory only in connection with a contact operator that corresponds to the range parameter $\beta \to \infty$.

The latter may acquire additional contributions from various heavy-meson exchanges that are allowed between the $D$ and $\bar{D}^*$ mesons. Therefore, the hierarchy of the scales relevant to the radiative decays of the $X(3872)$ is in fact provided by case B in Equation (12). Following the discussion in Section 3 above and substituting the momentum-space wave function in Equation (14) into the vertex in Equation (22), one concludes that the decay vertex $X(3872) \to D\bar{D}^*$ can be taken as a constant that drops out from the ratio in Equation (31). Thus, no overlap of the deuteron-like wave function in Equation (13) with anything else can drive the ratio $\mathcal{R}_X$ in Equation (31) as a matter of principle, contrary to the claim in ref. [33]. Instead, the loop amplitudes depicted in Figure 7a–e need to be evaluated. The

result of this calculation reported in ref. [44] (see also an update contained in ref. [45] and a similar calculation in ref. [46])

(i) Shows that the mechanism of the radiative decays of the $X(3872)$, assumed to be a $D\bar{D}^*$ molecule, does not imply light-quark pair annihilation, as considered in ref. [33], since the photon is emitted electrically or magnetically from a $D^{(*)}$ meson in the loop.

(ii) Implies that, even for a purely $D\bar{D}^*$ molecule assignment for the $X(3872)$, the ratio in Equation (31) can be of the order of unity under a not restrictive assumption for the couplings of the vector charmonia $J/\psi$ and $\psi(2S)$ to the $D^{(*)}$ mesons being numerically close to each other. (Since both $J/\psi$ and $\psi(2S)$ lie below the open-charm threshold, these couplings cannot be evaluated from the corresponding decay widths. Meanwhile, since the $\psi(2S)$ has a larger mass and therefore lies closer to the relevant open-charm thresholds, the corresponding couplings are expected to somewhat exceed those inherent in the $J/\psi$ that lies lower in the spectrum of charmonium and, therefore, further from the open-charm thresholds.)

(iii) Demonstrates a sizeable dependence of the ratio in Equation (31) on the renormalisation scale $\mu_{\rm ren}$ introduced by the regularisation procedure applied to the divergent loop amplitudes. In particular,

$$\delta R_{\rm mol}(\mu_{\rm ren}) \simeq R_{\rm mol}(\mu_{\rm ren}), \tag{36}$$

for $\mu_{\rm ren}$ varied in the range from $m_X/2$ to $2m_X$, with $m_X$ for the nominal $X$ mass.

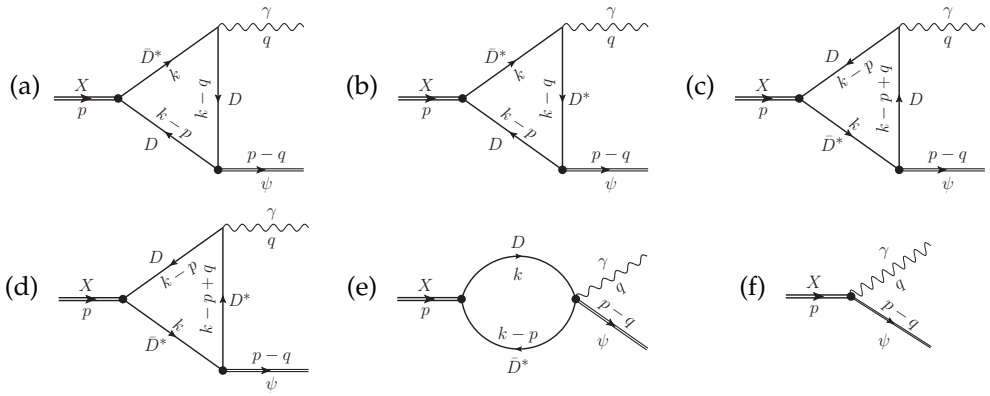


**Figure 7.** The diagrams (**a**–**f**) contributing to the amplitude of the decay $X(3872) \to \gamma\psi$ with $\psi = J/\psi$, $\psi(2S)$. Adapted from ref. [44].

The latter conclusion above is naturally interpreted then as a signal of sensitivity of the ratio $\mathcal{R}_X$ to the short-range physics encoded in the additional contact diagram depicted in Figure 7f. The corresponding short-range interaction needs to absorb the dependence of the decay amplitude on $\mu_{\rm ren}$ to ensure that the total result is consistent with the renormalisation group equation $\partial\mathcal{R}_X/\partial\mu_{\rm red} = 0$. In particular, Equation (36) implies that the contribution from the compact component given by the diagram in Figure 7f should be at least of the same size as the "molecular" contribution coming from the diagrams in Figure 7a–e. However, no further quantitative conclusion on the nature of the $X(3872)$ can be deduced from this calculation, since a scheme-independent separation of the contributions to the ratio in Equation (31) coming from the compact and molecular components is not possible as a matter of principle. Thus one is forced to conclude that the radiative decays of the $X(3872)$ are sensitive to the short-range component of the $X$ wave function and as such are out of control in the effective field theory framework for the $X$. In other words, the ratio $\mathcal{R}_X$ in Equation (31) is not decisive in establishing the nature of the $X(3872)$ (assuming the radiative decays of the $X(3872)$ proceed through the short-range component of its

wave function one can naturally arrive at the experimental ratio in Equation (31)—see, for example, refs. [44,47]). One the other hand, the radiative decays $Y(4260) \to \gamma X(3872)$ that involve the $X(3872)$ in the final state are sensitive to its molecular component [48].

To conclude this section, it is instructive to compare the case of the $X$ radiative decays studied here to the decays addressed in the previous sections. On the one hand, unlike the $D_{s1} \to \gamma D_{s0}^*$ decay in Section 4, only one molecular state is involved in the process $X \to \gamma\psi$. Moreover, the charmonium $\psi$ is not selective in its coupling to the various $D^{(*)}\bar{D}^{(*)}$ pairs, which appears to be in $P$-wave and therefore brings an extra power of the loop momentum. As a result, photon emission vertices of both electric and magnetic types contribute to the total amplitude. In the meantime, to preserve parity, the coupling of the $X$ to $\gamma\psi$ has to be anomalous and involves the field tensor for the electromagnetic field,

$$\mathcal{L}_{\text{eff}} = g_{X\psi\gamma}\epsilon_{\mu\nu\sigma\lambda}X^\mu\psi^\nu F^{\sigma\lambda}. \tag{37}$$

It automatically guarantees gauge invariance of the amplitude and, therefore, the latter does not call for the delicate cancellations between the different parts of the amplitude to form a transverse structure as discussed in Section 2. As a result, the amplitude of the decay $X \to \gamma\psi$ diverges while staying consistent with gauge invariance. This marks the crucial difference between the radiative $X$ decays and the cases of the radiative decays that were addressed in Sections 2 and 3.

## 6. Conclusions

In this paper, we reviewed various radiative decays involving hadronic molecules and stressed that information on such decays can provide valuable insight into their nature. However, one has to bear in mind that

(i) The hierarchy of the scales relevant to the studied hadron plays a crucial role—sticking to a wrong hierarchy will result in a misinterpretation of the information contained in the experimental data;

(ii) Different radiative decays may be sensitive to different components of the wave function of the studied hadron, so probing its long-range molecular component requires a careful choice of the observables to employ.

We provided several examples of the radiative decays that involve various strong candidates for hadronic molecules, illustrating the general pattern just outlined. In particular, we argue that a typical hierarchy of the scales inherent in hadronic molecules precludes employing the positronium-like formula based on $\psi(0)$ for their two-photon decays. Instead, the molecule disintegration vertex to its constituents should be taken as a constant obtained either employing the Weinberg formula or, more generally, derived from the residue of the corresponding scattering amplitude at the pole. After that, the loop diagrams that arise for a considered radiative decay need to be evaluated employing the standard field theory technique. Then one of the following three situations can take place:

- The decay amplitude contains convergent loop integrals and the power counting shows no need for a contact diagram. The width of such radiative decay can be evaluated without unknown parameters and then, as a prediction, confronted with the existing experimental data. This way the data allow one to probe the molecular nature of the hadronic state under study. The given situation is well exemplified with the radiative decays $S \to \gamma\gamma$ and $\phi(1020) \to \gamma S$ (with $S = a_0/f_0(980)$ treated as $K\bar{K}$ molecules) discussed in Sections 2 and 3.
- The decay amplitude contains convergent loop integrals but the power counting demonstrates no enhancement of the loop diagrams over a contact one. Then a contact term needs to be added to the effective Lagrangian with an unknown coefficient.

https://doi.org/10.3390/particles9020046

In this case, experimental data need to be employed first to fix the strength of the contact interaction. The radiative decay $D_{s1}(2460) \to \gamma D_{s0}^*(2317)$, with both $D_{sJ}$ mesons treated as $D^{(*)}K$ molecules, addressed in Section 4 provides an example of this pattern. It is expected that, once the strength of the contact interaction is fixed in the experiment, further predictions become possible for various reactions involving the vertex $D_{s1}D_{s0}^*\gamma$ as a building block or related to it via heavy quark symmetry.

- The decay amplitude contains divergent loop integrals and, therefore, requires a contact diagram already at leading order. The strength of the corresponding contact term can be estimated from its scheme dependence and, if the latter is strong, one is forced to conclude that the studied radiative decay is sensitive to the short-range component of the wave function of the decaying state rather than its long-range molecular one. In this case, experimental studies of this radiative decay do not allow one to probe the molecular nature of the state in question. Such a situation is well exemplified by the radiative decays $X(3872) \to \gamma\psi$ (with $\psi = J/\psi, \psi(2S)$) addressed in Section 5.

We conclude, therefore, that (i) identification of the hierarchy of the scales inherent to the studied molecule candidate, (ii) establishment of the power counting relevant to various contributions to its decay amplitude, and (iii) verification of the convergence and scheme dependence of the loop integrals involved are the necessary prerequisites that allow one to unambiguously judge whether or not the studied radiative decays can probe the nature of the given hadronic state.

**Author Contributions:** F.-K.G., C.H. and A.N.; formal analysis, F.-K.G., C.H. and A.N.; investigation, F.-K.G., C.H. and A.N.; writing—original draft preparation, F.-K.G.; writing—review and editing, F.-K.G., C.H. and A.N. All authors have read and agreed to the published version of the manuscript.

**Funding:** This work is supported in part by the National Key R&D Program of China under Grant No. 2023YFA1606703; by the Chinese Academy of Sciences (CAS) under Grant No. YSBR-101; and by the National Natural Science Foundation of China (NSFC) under Grants No. 12125507, No. 12361141819, and No. 12447101. The work of A.N. was supported by the Deutsche Forschungsgemeinschaft (Project No. 525056915). A.N. and C.H. also acknowledge support from the CAS President's International Fellowship Initiative (PIFI) (Grants No. 2024PVA0004_Y1 and No. 2025PD0087).

**Data Availability Statement:** No new data were used or produced in this research.

**Conflicts of Interest:** The authors declare no conflicts of interest.

## References

1. Guo, F.K.; Hanhart, C.; Meißner, U.G.; Wang, Q.; Zhao, Q.; Zou, B.S. Hadronic molecules. *Rev. Mod. Phys.* **2018**, *90*, 015004. Erratum in *Rev. Mod. Phys.* **2022**, *94*, 029901. [CrossRef]
2. Barnes, T. Two Photon Decays Support the (K anti-K) Molecule Picture of the S* (975) and Delta (980). *Phys. Lett. B* **1985**, *165*, 434–440. [CrossRef]
3. Krewald, S.; Lemmer, R.H.; Sassen, F.P. Lifetime of kaonium. *Phys. Rev. D* **2004**, *69*, 016003. [CrossRef]
4. Hanhart, C.; Kalashnikova, Y.S.; Kudryavtsev, A.E.; Nefediev, A.V. Two-photon decays of hadronic molecules. *Phys. Rev. D* **2007**, *75*, 074015. [CrossRef]
5. Nogga, A.; Hanhart, C. Can one extract the pi-neutron scattering length from pi-deuteron scattering? *Phys. Lett. B* **2006**, *634*, 210–213. [CrossRef]
6. Mori, T.; Uehara, S.; Watanabe, Y.; Abe, K.; Adachi, I.; Aihara, H.; Anipko, D.; Arinstein, K.; Aulchenko, V.; Bakich, A.M.; et al. High statistics study of $f_0(980)$ resonance in $\gamma\gamma \to \pi^+\pi^-$ production. *Phys. Rev. D* **2007**, *75*, 051101. [CrossRef]
7. Close, F.E.; Isgur, N.; Kumano, S. Scalar mesons in phi radiative decay: Their implications for spectroscopy and for studies of CP violation at phi factories. *Nucl. Phys. B* **1993**, *389*, 513–533. [CrossRef]
8. Achasov, N.N.; Gubin, V.V.; Shevchenko, V.I. Production of scalar K anti-K molecules in phi radiative decays. *Phys. Rev. D* **1997**, *56*, 203–211. [CrossRef]

9. Achasov, N.N.; Kiselev, A.V. Once more about the K anti-K molecule approach to the light scalars. *Phys. Rev. D* **2007**, *76*, 077501. [CrossRef]
10. Kalashnikova, Y.S.; Kudryavtsev, A.E.; Nefediev, A.V.; Hanhart, C.; Haidenbauer, J. The Radiative decays $\phi \to \gamma a_0/f_0$ in the molecular model for the scalar mesons. *Eur. Phys. J. A* **2005**, *24*, 437–443. [CrossRef]
11. Kalashnikova, Y.S.; Kudryavtsev, A.E.; Nefediev, A.V.; Haidenbauer, J.; Hanhart, C. Comment on 'Once more about the $K\bar{K}$ molecule approach to the light scalars'. *Phys. Rev. D* **2008**, *78*, 058501. [CrossRef]
12. Weinberg, S. Evidence That the Deuteron Is Not an Elementary Particle. *Phys. Rev.* **1965**, *137*, B672–B678. [CrossRef]
13. Achasov, N.N.; Ivanchenko, V.N. On a Search for Four Quark States in Radiative Decays of phi Meson. *Nucl. Phys. B* **1989**, *315*, 465–476. [CrossRef]
14. Barnes, T.; Close, F.E.; Lipkin, H.J. Implications of a $DK$ molecule at 2.32-GeV. *Phys. Rev. D* **2003**, *68*, 054006. [CrossRef]
15. Kolomeitsev, E.E.; Lutz, M.F.M. On Heavy light meson resonances and chiral symmetry. *Phys. Lett. B* **2004**, *582*, 39–48. [CrossRef]
16. Chen, Y.Q.; Li, X.Q. A Comprehensive four-quark interpretation of $D_s(2317)$, $D_s(2457)$ and $D_s(2632)$. *Phys. Rev. Lett.* **2004**, *93*, 232001. [CrossRef]
17. Guo, F.K.; Shen, P.N.; Chiang, H.C.; Ping, R.G.; Zou, B.S. Dynamically generated $0^+$ heavy mesons in a heavy chiral unitary approach. *Phys. Lett. B* **2006**, *641*, 278–285. [CrossRef]
18. Guo, F.K.; Shen, P.N.; Chiang, H.C. Dynamically generated $1^+$ heavy mesons. *Phys. Lett. B* **2007**, *647*, 133–139. [CrossRef]
19. Gamermann, D.; Oset, E.; Strottman, D.; Vicente Vacas, M.J. Dynamically generated open and hidden charm meson systems. *Phys. Rev. D* **2007**, *76*, 074016. [CrossRef]
20. Lutz, M.F.M.; Soyeur, M. Radiative and isospin-violating decays of $D_s$-mesons in the hadrogenesis conjecture. *Nucl. Phys. A* **2008**, *813*, 14–95. [CrossRef]
21. Faessler, A.; Gutsche, T.; Lyubovitskij, V.E.; Ma, Y.L. Strong and radiative decays of the $D^*_{s0}(2317)$ meson in the DK-molecule picture. *Phys. Rev. D* **2007**, *76*, 014005. [CrossRef]
22. Fu, H.L.; Guo, F.K.; Hanhart, C.; Nefediev, A. What can we learn from the radiative decays of the $D_{s1}(2460)$ meson? *arXiv* **2025**, arXiv:2512.05476. [CrossRef]
23. Fu, H.L.; Grießhammer, H.W.; Guo, F.K.; Hanhart, C.; Meißner, U.G. Update on strong and radiative decays of the $D^*_{s0}(2317)$ and $D_{s1}(2460)$ and their bottom cousins. *Eur. Phys. J. A* **2022**, *58*, 70. [CrossRef]
24. Bardeen, W.A.; Eichten, E.J.; Hill, C.T. Chiral Multiplets of Heavy–Light Mesons. *Phys. Rev. D* **2003**, *68*, 054024. [CrossRef]
25. Navas, S.; Amsler, C.; Gutsche, T.; Hanhart, C.; Hernández-Rey, J.J.; Lourenço, C.; Masoni, A.; Mikhasenko, M.; Mikhasenko, R.E.; Anderson , J.; et al. Review of particle physics. *Phys. Rev. D* **2024**, *110*, 030001. [CrossRef]
26. Cleven, M.; Grießhammer, H.W.; Guo, F.K.; Hanhart, C.; Meißner, U.G. Strong and radiative decays of the $D^*_{s0}(2317)$ and $D_{s1}(2460)$. *Eur. Phys. J. A* **2014**, *50*, 149. [CrossRef]
27. Cleven, M. Systematic Study of Hadronic Molecules in the Heavy-Quark Sector. Ph.D. Thesis, University of Bonn, Bonn, Germany, 2013.
28. Aaij, R.; Abdelmotteleb, A.S.W.; Abellan Beteta, C.; Abudinén, F.; Ackernley, T.; Adefisoye, A.A.; Adeva, B.; Adinolfi, M.; Adlarson, P.; Agapopoulou, C.; et al. Probing the nature of the $\chi_{c1}(3872)$ state using radiative decays. *J. High Energy Phys.* **2024**, *11*, 121. [CrossRef]
29. LHCb Collaboration. Evidence for the decay $X(3872) \to \psi(2S)\gamma$. *Nucl. Phys. B* **2014**, *886*, 665–680. [CrossRef]
30. Aubert, B.; Bona, M.; Karyotakis, Y.; Lees, J.P.; Poireau, V.; Prencipe, E.; Prudent, X.; Tisserand, V.; Tico, J.G.; Grauges, E.; et al. Evidence for $X(3872) \to \psi_{2S}\gamma$ in $B^\pm \to X_{3872}K^\pm$ decays, and a study of $B \to c\bar{c}\gamma K$. *Phys. Rev. Lett.* **2009**, *102*, 132001. [CrossRef] [PubMed]
31. Choi, S.K.; Olsen, S.L.; Abe, K.; Abe, T.; Adachi, I.; Ahn, B.S.; Aihara, H.; Akai, K.; Akatsu, M.; Akemoto, M.; et al. Observation of a narrow charmonium-like state in exclusive $B^\pm \to K^\pm\pi^+\pi^- J/\psi$ decays. *Phys. Rev. Lett.* **2003**, *91*, 262001. [CrossRef]
32. Swanson, E.S. Diagnostic decays of the $X(3872)$. *Phys. Lett. B* **2004**, *598*, 197–202. [CrossRef]
33. Grinstein, B.; Maiani, L.; Polosa, A.D. Radiative decays of $X(3872)$ discriminate between the molecular and compact interpretations. *Phys. Rev. D* **2024**, *109*, 074009. [CrossRef]
34. Bhardwaj, V.; Trabelsi, K.; Singh, J.B.; Choi, S.-K.; Olsen, S.L.; Adachi, I.; Adamczyk, K.; Asner, D.M.; Aulchenko, V.; Aushev, Y.; et al. Observation of $X(3872) \to J/\psi\gamma$ and search for $X(3872) \to \psi'\gamma$ in $B$ decays. *Phys. Rev. Lett.* **2011**, *107*, 091803. [CrossRef]
35. Ablikim, M.; Achasov, M.N.; Adlarson, P.; Ahmed, S.; Albrecht, M.; Amoroso, A.; An, Q.; Anita; Bai, Y.; Bakina, Q.; et al. Study of Open-Charm Decays and Radiative Transitions of the $X(3872)$. *Phys. Rev. Lett.* **2020**, *124*, 242001. [CrossRef]
36. Aaij, R.; Beteta, C.A.; Adeva, B.; Adinolfi, M.; Adrover, C.; Affolder, A.; Ajaltouni, Z.; Albrecht, J.; Alessio, F.; Alexander, M.; et al. Determination of the $X(3872)$ meson quantum numbers. *Phys. Rev. Lett.* **2013**, *110*, 222001. [CrossRef]
37. Aaij, R.; Adeva, B.; Adinolfi, M.; Affolder, A.; Ajaltouni, Z.; Akar, S.; Albrecht, J.; Alessio, F.; Alexander, M.; Ali, S.; et al. Quantum numbers of the $X(3872)$ state and orbital angular momentum in its $\rho^0 J\psi$ decay. *Phys. Rev. D* **2015**, *92*, 011102. [CrossRef]
38. Ji, T.; Dong, X.K.; Guo, F.K.; Hanhart, C.; Meißner, U.G. Precise determination of the properties of $X(3872)$ and of its isovector partner $W_{c1}$. *arXiv* **2025**, arXiv:2502.04458. [CrossRef]

39. Baru, V.; Filin, A.A.; Hanhart, C.; Kalashnikova, Y.S.; Kudryavtsev, A.E.; Nefediev, A.V. Three-body $D\bar{D}\pi$ dynamics for the $X(3872)$. *Phys. Rev. D* **2011**, *84*, 074029. [CrossRef]
40. Tornqvist, N.A. From the deuteron to deusons, an analysis of deuteron-like meson meson bound states. *Z. Phys. C* **1994**, *61*, 525–537. [CrossRef]
41. Swanson, E.S. Short range structure in the $X(3872)$. *Phys. Lett. B* **2004**, *588*, 189–195. [CrossRef]
42. Suzuki, M. The $X(3872)$ boson: Molecule or charmonium. *Phys. Rev. D* **2005**, *72*, 114013. [CrossRef]
43. Baru, V.; Epelbaum, E.; Filin, A.A.; Guo, F.K.; Hammer, H.W.; Hanhart, C.; Meißner, U.G.; Nefediev, A.V. Remarks on study of $X(3872)$ from effective field theory with pion-exchange interaction. *Phys. Rev. D* **2015**, *91*, 034002. [CrossRef]
44. Guo, F.K.; Hanhart, C.; Kalashnikova, Y.S.; Meißner, U.G.; Nefediev, A.V. What can radiative decays of the $X(3872)$ teach us about its nature? *Phys. Lett. B* **2015**, *742*, 394–398. [CrossRef]
45. Shi, P.P.; Dias, J.M.; Guo, F.K. Radiative decays of the spin-2 partner of $X(3872)$. *Phys. Lett. B* **2023**, *843*, 137987. [CrossRef]
46. Molnar, D.A.S.; Luiz, R.F.; Higa, R. Short-distance RG-analysis of $X(3872)$ radiative decays. *arXiv* **2016**, arXiv:1601.03366. [CrossRef]
47. Brambilla, N.; Mohapatra, A.; Scirpa, T.; Vairo, A. Nature of $\chi_c 1(3872)$ and $T_{cc}^{+}(3875)$. *Phys. Rev. Lett.* **2025**, *135*, 131902. [CrossRef] [PubMed]
48. Guo, F.K.; Hanhart, C.; Meißner, U.G.; Wang, Q.; Zhao, Q. Production of the $X(3872)$ in charmonia radiative decays. *Phys. Lett. B* **2013**, *725*, 127–133. [CrossRef]